Proceedings of the 6th JFPS International
Symposium on Fluid Power, TSUKUBA 2005
November 7-10, 2005

RELATIONSHIP BETWEEN OSCILLATION FREQUENCY AND GEOMETRY OF OSCILLATING LPA FLOW SENSOR

Hisaki SHIMIZU*, Fujio HIROKI** and Keijiro YAMAMOTO***

* Department of Intelligent Systems Engineering
Ichinoseki National College of Technology
Takanashi ,Hagisyo, Ichinoseki, Iwate, 021-8511 Japan
(E-mail shimiz6@ichinoseki.ac.jp)
**Department of Mechanical Systems Engineering, Faculty of Engineering
Kogakuin University
2665 Nakanocho, Hachiouji, Tokyo, 192-0015 Japan
***Department of Welfare Systems Engineering, Faculty of Engineering
Kanagawa Institute of Technology
1030 Shimoogino, Atsugi, Kanagawa, 243-0292 Japan

ABSTRACT

The oscillating LPA(Laminar Proportional Amplifier) flow sensor having bilateral feedback loops is available for the measurement of small volume flow. Pattern of LPA and feedback loops were sculpted on a flat plane. The relationship between the oscillating frequency and the geometry of the oscillating LPA flow sensors were measured. As the result of experiments, it was appeared that the oscillating frequency of the oscillating LPA flow sensor closely connected with the geometry and the sizes of the sensor, and the signal transport time through the feedback loop was about a half of the acoustic time delay, and it was proved that the signal transport time on the supply jet from the supply nozzle to the splitter were occupied about 60% of the oscillating frequency. It was demonstrated that the range ability of the oscillating LPA flow sensor could be extended by arranging the pattern of LPA and feedback loops in the same plane.

KEY WORDS

Laminar proportional amplifier, flow sensor, feedback oscillator, frequency, geometry

1. INTRODUCTION

The oscillating LPA flow sensor utilizing Laminar Proportional Amplifier (LPA) is available for the measurement of the small volume flow. In previous papers[1), 2), 3)], we clarified that the oscillating frequency of the oscillating LPA flow sensor closely connected with the geometry and the sizes of the pattern of LPA and that of feedback channels. In this study, we investigate the oscillation mechanism of the feedback oscillator utilizing LPA.

2. GEOMETRY OF THE OSCILLATING LPA FLOW SENSOR

Figure 1 shows a schematic diagram of feedback oscillator utilizing a LPA which consists of LPA and bilateral feedback loops. This oscillator is available for the measurement of the small volume flow, because LPA is operated efficiently under the condition of low Reynolds number, i.e., laminar flow.

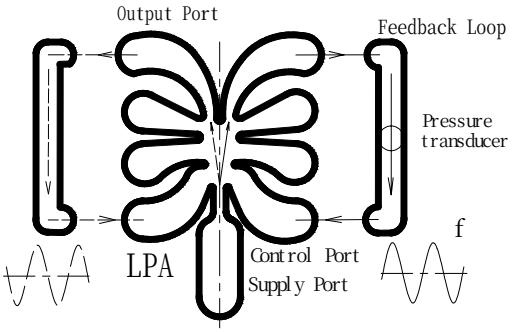

Figure 1 Geometry of LPA flow sensor

The jet goes out through one of the output ports, by feeding back a part of the jet flow, periodic oscillation of the jet between the feedback loops can be achieved. The oscillating pressure signals at the output ports were measured by using condenser type microphones. The oscillation frequency was measured by using FFT analyzer.

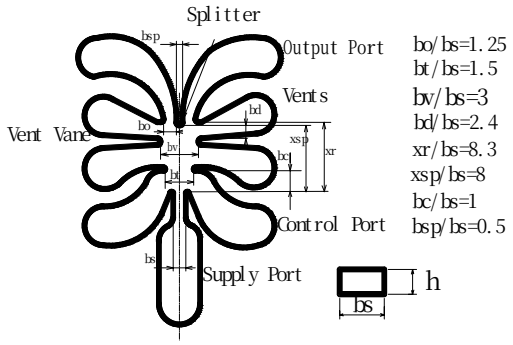

Figure 2 Geometry of LPA

Figure 2 shows a schematic diagram and major dimensions of LPA normalized by supply nozzle width.
The material of the flow sensors is thin stainless steel. They were manufactured by an electric discharge machine. The flow sensors were sandwiched by two covering plates made of brass. In this study, air was used as a working fluid.
We manufactured two type flow sensors. Figure 3 shows the geometry of the flow sensor (1), which consists of LPA and bilateral feedback loops of round tubes(sections of a oblique line in the figure).

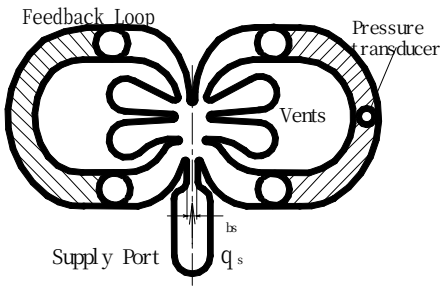

Figure 3 Geometry of flow sensor (1)

Figure 4 shows geometry of oscillating flow sensor (2) which arranged the ports of LPA and feedback loops in same plane.

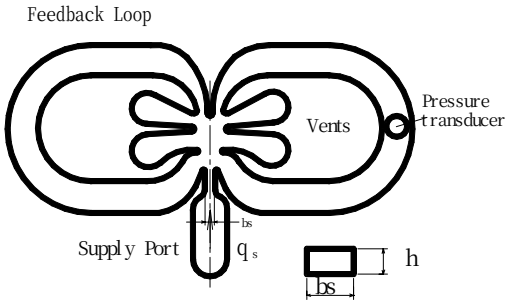

Figure 4 Geometry of oscillating flow sensor (2)

3. FREQUENCY - FLOW RELATIONSHIP

Figure 5 shows comparison of the frequency-flow (f-q_s) characteristics of sensor (1) and sensor (2). The height and width of the supply nozzle of the sensor (1) and sensor (2) were 0.75mm and 0.8mm, respectively.

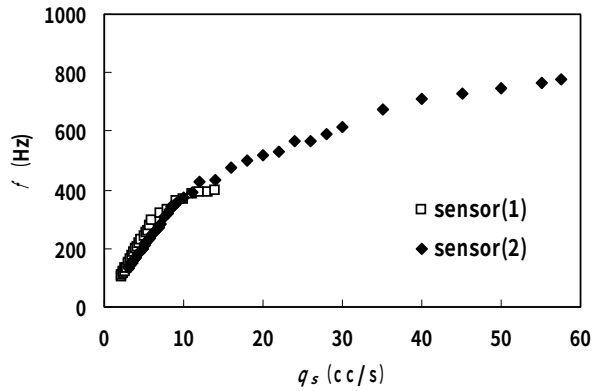

Figure 5 f-q_s Characteristics of sensor (1) and sensor (2)

In the case of sensor (1), sizes of the round feedback loop are the diameter D=4mm and the length L=172mm. In the case of sensor (2), sizes of the rectangular feedback loop are width b_f=2.4mm, depth h_f=0.8mm and the length L=48mm. The frequency increases proportionally to the volumetric flow rate of supply jet within low flow range up to the breaking point. In the case of sensor (1), there are the lower limit of flow rate for the oscillation at 2.2cc/s and the upper limit of flow for the oscillation at 15cc/s, and the breaking point is 8cc/s.
In the case of sensor (2), there are the lower limit of flow for the oscillation at 3cc/s and the upper limit of flow for the oscillation at 60cc/s, and the breaking point is 12cc/s . In the case of sensor (2), the thin feedback loops has a highly inhibitory action against the flow turbulent. This results show that the structure arranging the pattern of LPA and feedback loops in the same plane have the

effect to expand oscillating flow range.

4. EASUREMENTS OF PRESSURE TRANSMISSION AND PROPAGATION PERIOD

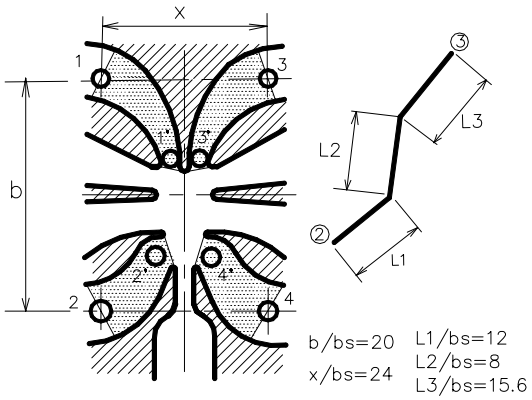

Figure 6 Points of measurement

To clarify the relationship between the oscillation frequency and the geometry of the sensor, pressure signal transport times between specific points were measured. Points of measurement are shown in figure 6. Figure 7 shows the conjectural propagation lengths.

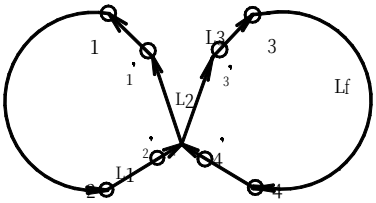

Figure 7 Conjectural propagation lengths

Oscillation frequency f can be appeared as follows,

$$f = 1 / total \quad \cdots\cdots\cdots\cdots (1)$$

$$total = t_{12} + t_{23} + t_{34} + t_{41} \quad \cdots\cdots\cdots\cdots (2)$$

$$t_{23} = t_{22'} + t_{2'3'} + t_{3'3} \quad \cdots\cdots\cdots\cdots (3)$$

$$t_{41} = t_{44'} + t_{4'1'} + t_{1'1} \quad \cdots\cdots\cdots\cdots (4)$$

where *total* is the period i.e. total time required for pressure signal propagates one round, t_{12} is the signal transport time from point 1 to point 2 of the left-hand feedback loop, t_{23} is the signal transport time from point 2 to point 3, t_{34} is the signal transport time from point 3 to point 4 of the right-hand feedback loop, t_{41} is the signal transport time from point 4 to point 1, $t_{22'}$ is the signal transport time from point 2 to point 2' of the left-hand input nozzle, $t_{2'3'}$ is the signal transport time from point 2' to point 3', $t_{3'3}$ is the signal transport time from point 3' to point 3 of the right-hand output duct, $t_{44'}$ is the signal transport time from point 4 to point 4' of the right-hand input nozzle, $t_{4'1'}$ is the signal transport time from point 4' to point 1' and $t_{1'1}$ is the signal transport time from point 1' to point 1 of the left-hand output duct.

5. RESULTS AND DISCUSSION

5.1 FEEDBACK LOOP

The relationships between the signal transport time in the feedback loops for various lengths of the sensor (1), and volume flow rates are shown in Figure 8. The values on the ordinates are the mean value of t_{12} and t_{34}.

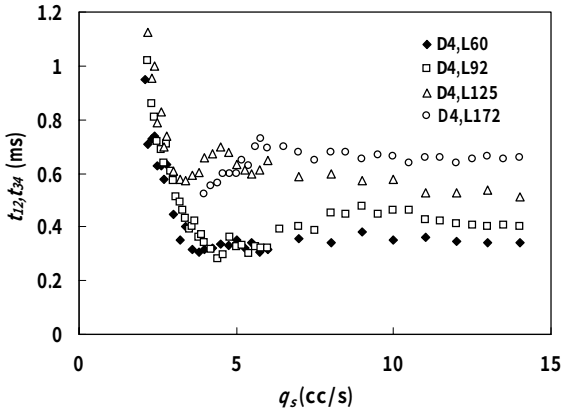

Figure 8 t_{12}, t_{34} versus q_s of sensor (1)

In case of the sensor (1), it was appeared that the signal transport times t_{12}, t_{34} decrease as flow increase in the small flow region under 3~4cc/s, on the other hand, they does not change in the region of flow above 3~4cc/s and they increase with the lengths of the feedback loop. Figure 9 shows the signal transport velocity, U_f versus volume flow, q_s. The value of U_f is calculated by the signal transport time in the both feedback loops and the length of them.

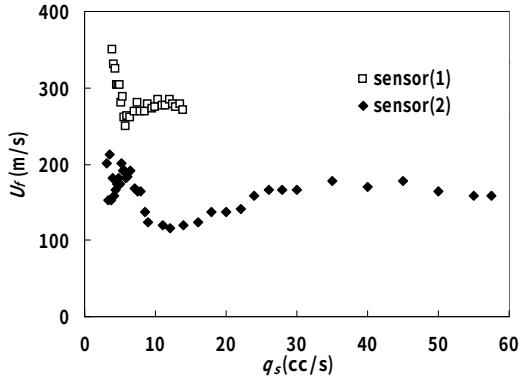

Figure 9 U_f versus q_s

In the case of the sensor (1), the signal transport velocity is nearly equal to the speed of sound in the small flow region. Bat in the sensor (2), the signal transport velocity is about half value of the speed of sound due to the effects of thin rectangular feedback loops.

5.2 INPUT NOZZLE

Figure 10 shows the signal transport time the both input nozzles, $t_{22'}$ $t_{44'}$ versus volume flow rates, q_s. In both sensors, the signal transport times $t_{22'}$ $t_{44'}$ decrease as flow increases in small flow region under 5cc/s, but they does not change in the region of flow above 6cc/s.

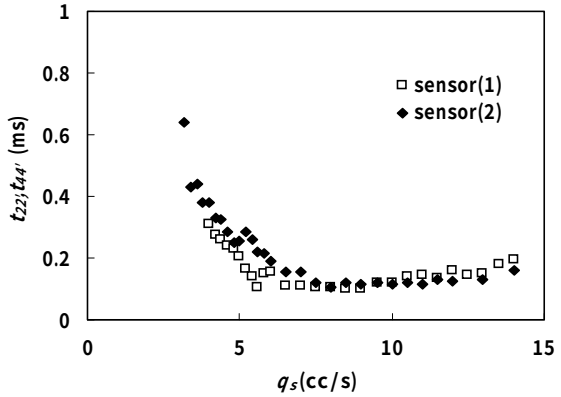

Figure 10 $t_{22'}$, $t_{44'}$ versus q_s

Figure 11 shows the signal transport velocity in the both input nozzles, U_1 versus volume flow, q_s. The value of U_1 is calculated by the signal transport time in the both input nozzles and the length of them. Since the length of the input nozzles was short, the signal transport velocity in the input nozzles is smaller than that of the feedback loops.

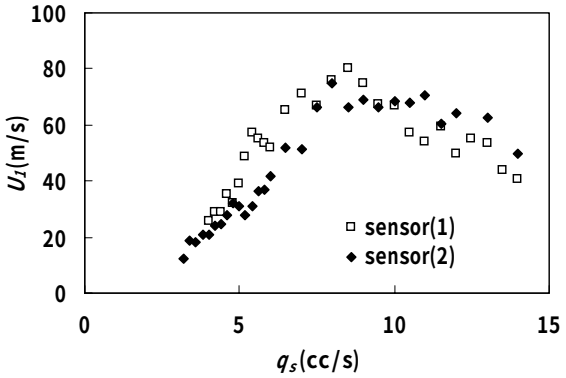

Figure 11 U_1 versus q_s

5.3 SUPPLY JET

Figure 12 shows the signal transport time of the supply jet, $t_{2'3'}$, $t_{4'1'}$ versus volume flow rates, q_s. In previous paper[4], the signal transport time through the supply jet, t_j was appeared as follows,

$$t_j = x_{sp} / 0.5U_s \cdots\cdots\cdots (5)$$

where x_{sp} is the distance between supply nozzle and splitter and U_s is the signal transport velocity through the supply jet. In both sensors, the signal transport time through the supply jet, $t_{2'3'}$, $t_{4'1'}$ are nearly equal to t_j. The signal transport time through the supply jet occupy the most of the oscillation period.

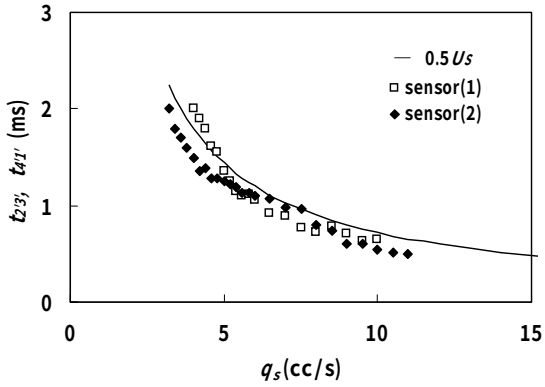

Figure 12 $t_{2'3'}$, $t_{4'1'}$ versus q_s

5.4 OUTPUT DUCT

Figure 13 shows the signal transport velocity in the both output ports, U_3 versus volume flow, q_s. The value of U_3 is calculated by the signal transport time in the both output ducts and the length of them. This signal transport velocity is smaller than the signal transport velocity in the feedback loops. The signal transport velocity increase proportionally with the volume flow within small flow region under 4~5cc/s .

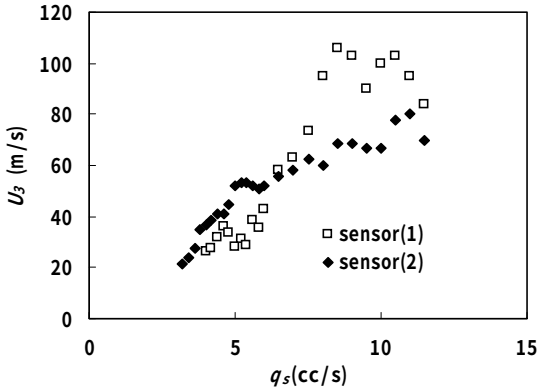

Figure 13 U_3 versus q_s

5.5 RELATIVE SIGNAL TRANSPORT TIMES

Figure 14 shows the ratio of the signal transport time, *t/total* versus volume flow, q_s of the sensor (2). t_f is the mean of t_{12} and t_{34}, t_1 is the mean of $t_{22'}$ and $t_{44'}$, t_2 is the mean of $t_{2'3'}$ and $t_{4'1'}$ and t_3 is the mean of $t_{1'1}$ and $t_{3'3}$. The signal transport time through the supply jet, t_2 occupy about 50% of the oscillation period under the flow of 8cc/s. The signal transport time in the feedback loops, t_f increase gradually as flow increase. t_1 and t_3 occupy about 15% of the oscillation period. Therefore, the oscillating frequency is affected considerably by the signal transport time through the supply jet. t_2 of the

sensor (1) showed similar tendency.

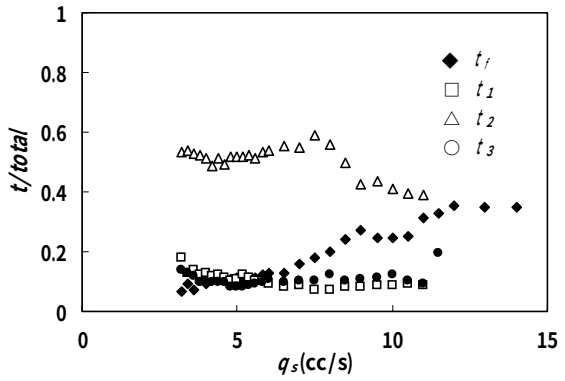

Figure 14 *t / total* versus q_s

6. CONCLUSION

The relationship between the oscillating frequency and the geometry of the oscillating LPA flow sensor were studied. Following conclusions were obtained.

1) The signal transport time through the feedback loops were affected considerably by the geometry of the feedback loop. The structure which arranged the ports of LPA and feedback loops in the same plane have the advantage in expanding working range.

2) The signal transport velocities in the input nozzle and in the output nozzle were smaller than that of the feedback loop.

3) The signal transport time from the supply nozzle to the splitter occupied about 60% of the oscillation period.

REFERENCES

1. Hisaki SHIMIZU and Keijiro YAMAMOTO: Characteristics of The Jet Deflection of Laminar Proportion Amplifiers, Papers of the 18th Sensing Forum, Soc. Instrum. & Control Eng., Japan, 2001. pp.95-98.
2. Hisaki SHIMIZU and Keijiro YAMAMOTO: Study of Oscillating LPA Flow Sensor (Characteristics of The Jet Deflection), Papers of the 19th Sensing Forum, Soc. Instrum. & Control Eng., Japan, 2002. pp.361-364.
3. Hisaki SHIMIZU, Masahiro CHIBA, Fujio HIROKI and Keijiro YAMAMOTO: Comparison of the Characteristics of Oscillating LPA Flow Sensor, Papers of the 20th Sensing Forum ,Soc. Instrum. & Control Eng., Japan, 2003. pp.105-108.
4. George Mon：A fluidic Volumetric-Flow, Mass Flow Density and Viscosity Meter, The Journal of Fluid Control, 1987. pp.7-18.